Ann. Rev. Earth Planet. Sci. 1987. 15: 245–70

TERRESTRIAL IMPACT STRUCTURES

Richard A. F. Grieve

Geophysics Division, Geological Survey of Canada, Ottawa, Ontario K1A 0Y3, Canada

INTRODUCTION

Impact structures are the dominant landform on planets that have retained portions of their earliest crust. The present surface of the Earth, however, has comparatively few recognized impact structures. This is due to its relative youthfulness and the dynamic nature of the terrestrial geosphere, both of which serve to obscure and remove the impact record. Although not generally viewed as an important terrestrial (as opposed to planetary) geologic process, the role of impact in Earth evolution is now receiving mounting consideration. For example, large-scale impact events may have been responsible for such phenomena as the formation of the Earth's moon and certain mass extinctions in the biologic record.

The importance of the terrestrial impact record is greater than the relatively small number of known structures would indicate. Impact is a highly transient, high-energy event. It is inherently difficult to study through experimentation because of the problem of scale. In addition, sophisticated finite-element code calculations of impact cratering are generally limited to relatively early-time phenomena as a result of high computational costs. Terrestrial impact structures provide the only ground truth against which computational and experimental results can be compared. These structures provide information on aspects of the third dimension, the pre- and postimpact distribution of target lithologies, and the nature of the lithologic and mineralogic changes produced by the passage of a shock wave. They also provide data for cratering rate estimates and, in some cases, on the nature of the impacting body.

In this review, emphasis is placed on the nature of terrestrial impact structures, the criteria for their identification, and their contribution to

0084–6597/87/0515–0245$02.00

constraining formational processes and cratering rate estimates. The relationship of large-scale impacts to Earth history is also considered. Further details of cratering mechanics, scaling relationships, and temporal aspects of the bombardment of the Earth can be found in reviews by Melosh (1980) and Shoemaker (1983).

BASIC CHARACTERISTICS

Although there are a number of research papers describing aspects of specific impact structures (Roddy et al 1977), there is unfortunately no single English language text that describes the basic geological and geophysical characteristics of terrestrial impact structures (cf. Masaitis et al 1980). These structures are characterized by a circular form and evidence for intense, localized, near-surface structural disturbance and brecciation. Geophysical modeling indicates that they do not have deep-seated roots. The disruption and brecciation lead to associated low seismic velocities and residual negative gravity anomalies (Pohl et al 1977). Their magnetic signature is often in the form of a disruption of the magnetic trends in the target rocks or a magnetic low (Dabizha & Ivanov 1978). Localized magnetic anomalies may also occur and have been attributed to a variety of impact and postimpact causes (Coles & Clark 1978). The principal criterion, however, for the recognition of an impact structure is the occurrence of so-called shock-metamorphic effects (French & Short 1968). These effects are largely related to the progressive destruction of mineral structure and to thermal effects associated with the passage of a shock wave.

Morphology

Terrestrial impact structures are subdivided into two morphological classes: simple and complex. Simple structures have the classic bowl shape exhibited by Meteor (Barringer) Crater, Arizona (Figure 1). They have an uplifted rim area, and in the freshest examples, this is overlain by an overturned flap of near-surface target rocks with inverted stratigraphy, which is in turn overlain by fallout ejecta. Drilling at a number of structures has indicated that the floor of the so-called apparent crater (Figure 1) is underlain by a lens of allochthonous unshocked and shocked target-rock breccia. Bounding the breccia lens are autochthonous brecciated and fractured target rocks. They define the so-called true crater, which is roughly parabolic in cross section (Figure 1). Shock-metamorphic effects in the autochthonous target rocks are limited to the lower wall and beneath the floor of the true crater (Figure 1). Simple structures have the morphometric

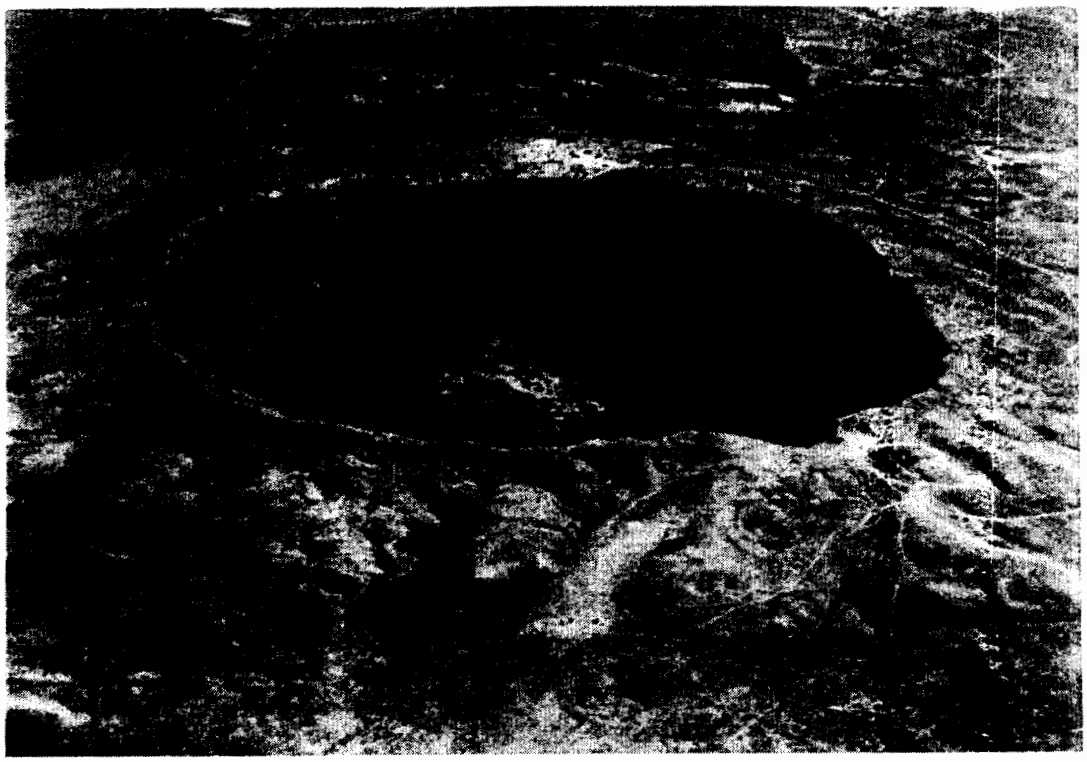

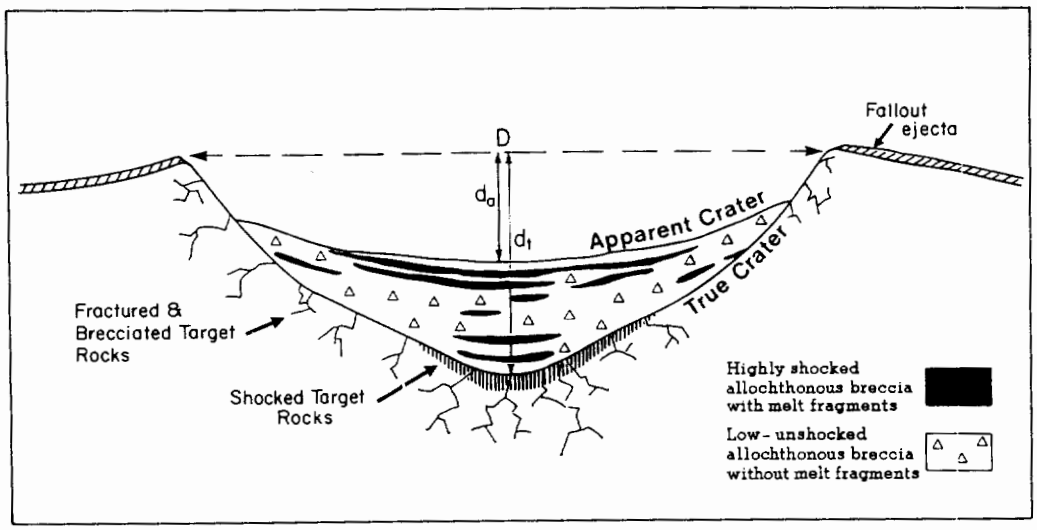

Figure 1 (*top*) Aerial photograph of Meteor (Barringer) Crater, Arizona, an example of a relatively young simple crater. (*bottom*) Schematic cross section of the principal elements of a simple crater in crystalline rocks. Notation defined in text.

relations

$$d_a = 0.14D^{1.02}, \qquad (n = 18;\ \text{Pike 1980})$$

and

$$d_t = 0.29D^{0.93}, \qquad (n = 9;\ \text{this work})$$

where D is the rim diameter, d_a and d_t are the apparent depth and true depth, respectively, n is the number of structures upon which the relation is based, and units are in kilometers (Figure 1). By comparison, lunar simple structures ($d_a = 0.196D^{1.01}$; Pike 1980) are deeper, reflecting the lower gravity of the Moon.

At diameters above ~2 km in sedimentary targets and ~4 km in crystalline targets, terrestrial impact structures have a complex form (Figure 2). The freshest examples are characterized by a structurally uplifted central area, exposed as a central peak and/or rings, surrounded by a peripheral depression and a faulted rim area. The peripheral depression is partly filled by allochthonous breccia and/or an annular sheet of so-called impact melt rocks. Shock-metamorphic effects in the autochthonous target rocks are present in the uplifted central area.

Various morphologic subtypes of complex structures identified on the other terrestrial planets [e.g. central peak craters, central peak basins, peak ring basins (Wood & Head 1976)] occur on Earth. Unequivocal terrestrial examples of multiring basins have not been identified. As many of the larger complex structures have been eroded to the extent that their principal morphologic elements are a mixture of structural and topographic features, morphometric comparisons with, for example, lunar structures (Pike 1985) should be made with caution. Complex structures are relatively shallow compared with simple structures, with the depth of the apparent crater given by

$$d_a = 0.27D^{0.16}, \qquad (n = 11;\ \text{Pike 1980}).$$

There is considerable uncertainty attached to this formulation (± 0.11 on the exponent; Pike 1980) due to scatter in the data, and other such relationships have been given. There is also some evidence that complex structures in sedimentary targets are systematically shallower than those in crystalline targets (Grieve et al 1981).

The principal difference between complex and simple structures is the occurrence of an uplifted central core of shocked target rocks in the latter. From structures with stratigraphic and structural control, it is possible to define

$$SU = 0.06D^{1.1}, \qquad (n = 10;\ \text{Grieve et al 1981})$$

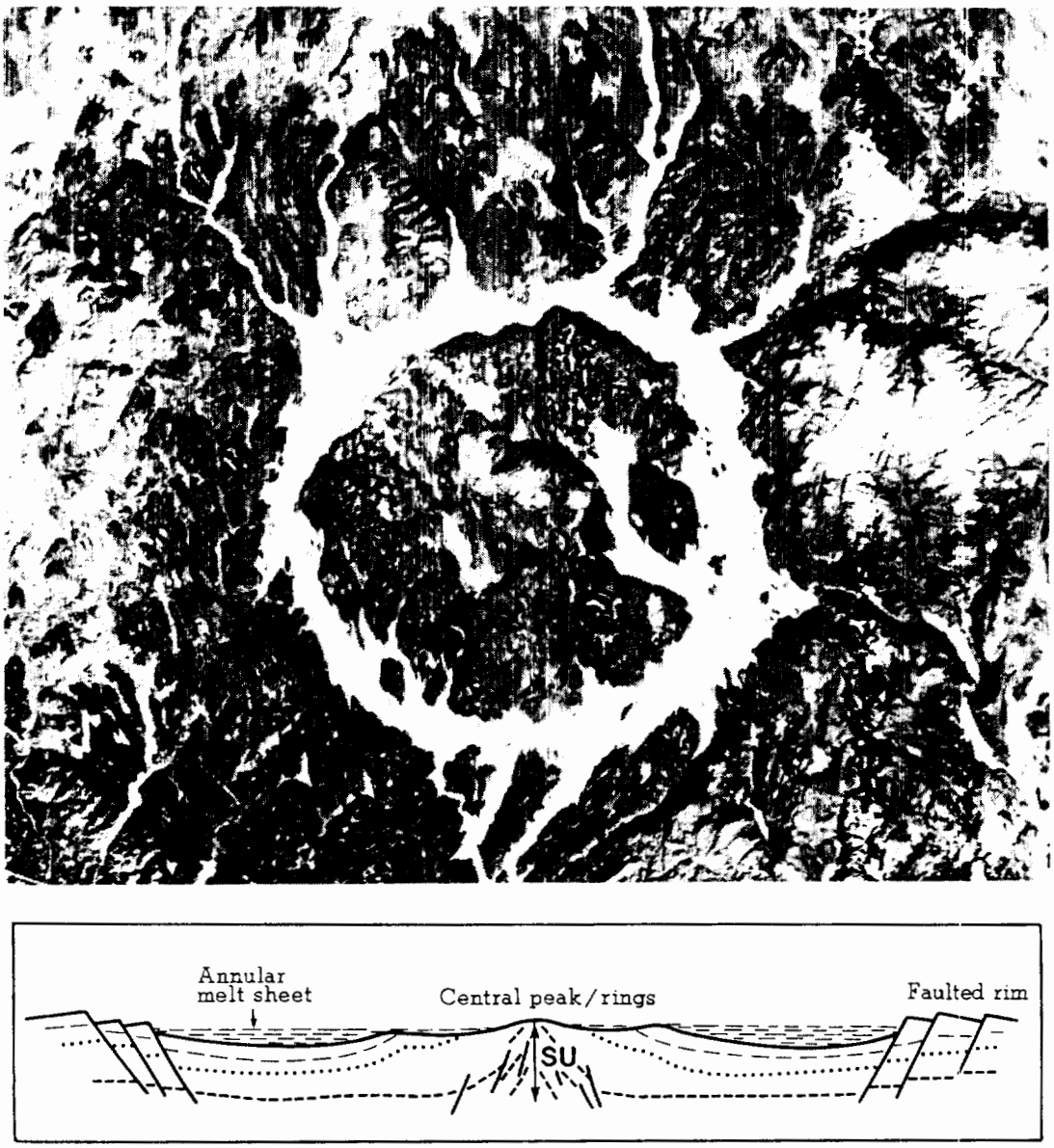

Figure 2 (*top*) LANDSAT image of the Manicouagan impact structure, Quebec, Canada. The annular lake has an outer diameter of ~70 km and surrounds an inner plateau capped by impact rocks and an uplifted central region. (*bottom*) Schematic cross section of the principal elements of a complex structure in crystalline rocks. Note the faulted rim area, the uplifted central area, and the relatively shallow nature compared with simple craters. The distance *SU* represents the net amount of structural uplift undergone by the deepest horizon now exposed in the central core.

where SU is the net amount of structural uplift undergone by the deepest horizon now exposed in the central core (Figure 2). This relationship is a minimum, as the amount of uplift decreases with depth (Brenan et al 1975) and erosion reduces the amount of observed uplift. It indicates, however, that an extensive vertical section of the upper crust is subjected to structural disturbance in the center of the largest structures (e.g. $SU \sim 9.5$ km for $D \sim 100$ km).

Shock Metamorphism

For typical terrestrial impact velocities of 15–25 km s^{-1}, the impacting body penetrates the target rocks to $\sim$2–3 times its radius and transfers the bulk of its kinetic energy to the target, where it is partitioned into kinetic and internal energy. Energy transfer is by means of a hemispherically propagating shock wave, which decays exponentially with radial distance until it becomes an elastic wave. The peak pressures occurring close to the point of impact are of the order of several hundred gigapascals or several megabars. Considerable pressure-volume work is done by shock compression. Not all of this is recovered on rarefaction, and some is trapped as waste heat. Close to the point of impact, the latter is sufficient to raise the temperature of the target to several thousand degrees Celsius. These high pressures and temperatures lead to a series of changes known as shock metamorphism in the minerals and rocks of the target. Shock metamorphism differs from traditional endogenic metamorphism in the scales of pressures, temperatures, and time (Figure 3). It is characterized by very high strain rates and disequilibrium. With increasing pressure, shock effects are manifested as fracturing and cataclasis, plastic deformation, phase transitions, thermal decomposition, melting, and finally vaporization. The subject of shock metamorphism is dealt with in detail in the volume edited by French & Short (1968) and in work by Stöffler (1972, 1974).

Above the Hugoniot elastic limit, which is in the range of 2–12 GPa for silicates (Stöffler 1972), material compressed by the shock wave is returned to ambient pressure with reduced density upon rarefaction and has permanent changes with respect to its initial preshock state. The reduction in postshock density is due to the progressive breakdown of crystallographic order with increasing pressure. The most detailed observational and experimental studies in shock metamorphism have been on the common rock-forming tectosilicates—quartz and feldspars—where the most obvious and best-documented characteristic is the occurrence of planar features (Figure 4*b*). These microscopic sets of planes, a few microns in width, correspond to glide planes now generally filled by solid-state glass (von Engelhardt & Bertsch 1969). Planar features develop along a few specific crystallographic orientations, and experimental studies indi-

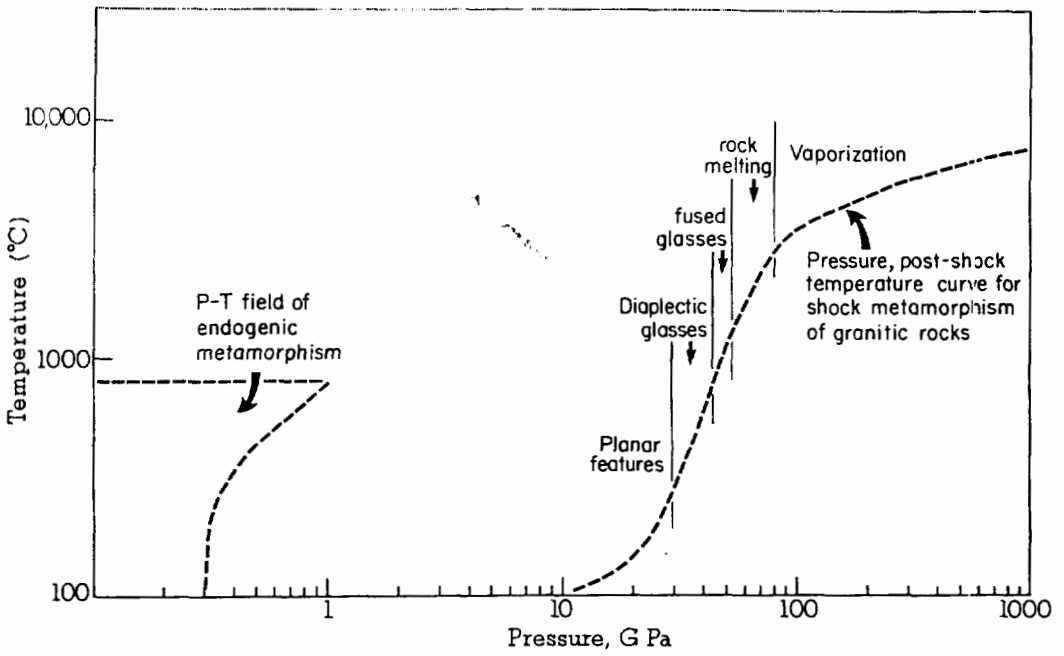

Figure 3 Pressure-temperature regime of shock metamorphism compared with that of endogenic metamorphism. Pressures and temperatures required for various shock-metamorphic features in granitic rocks are indicated.

cate that certain orientations develop in particular pressure ranges (Hörz 1968, Müller & Défourneaux 1968, Robertson 1975). Planar features in tectosilicates are developed over the range ~7.5–30 GPa, with the exact threshold pressure depending on mineral composition, structural state, exsolution lamellae, and alteration (Ostertag 1983). Accompanying planar feature development and with increasing shock pressure, there is increasing mosaicism, asterism, loss of birefringence, and glass formation. The only diagnostic megascopic shock feature in this general pressure range is a conical form of rock fracture known as shatter cones (Figure 4*a*). Although duplicated in experiments (Schneider & Wagner 1976, Roddy & Davis 1977), shatter-cone formation as a physical process has received little attention. These cones occur over a pressure range of 2–25 GPa, are developed best in fine-grained, structurally isotropic rocks, and are oriented with their apexes pointing in the direction of the origin of the shock wave (Milton 1977).

In the tectosilicates, there is a continuous structural change from crystals to glass, so that by ~30–45 GPa they are converted completely to so-called diaplectic glass (Stöffler & Hornemann 1972; Figure 4*c*). These solid-state glasses exhibit the original habit of the unshocked mineral and thus are also known as thetomorphic glasses. Metastable high-pressure polymorphs, such as stishovite, diamond, and other phases found on inversion

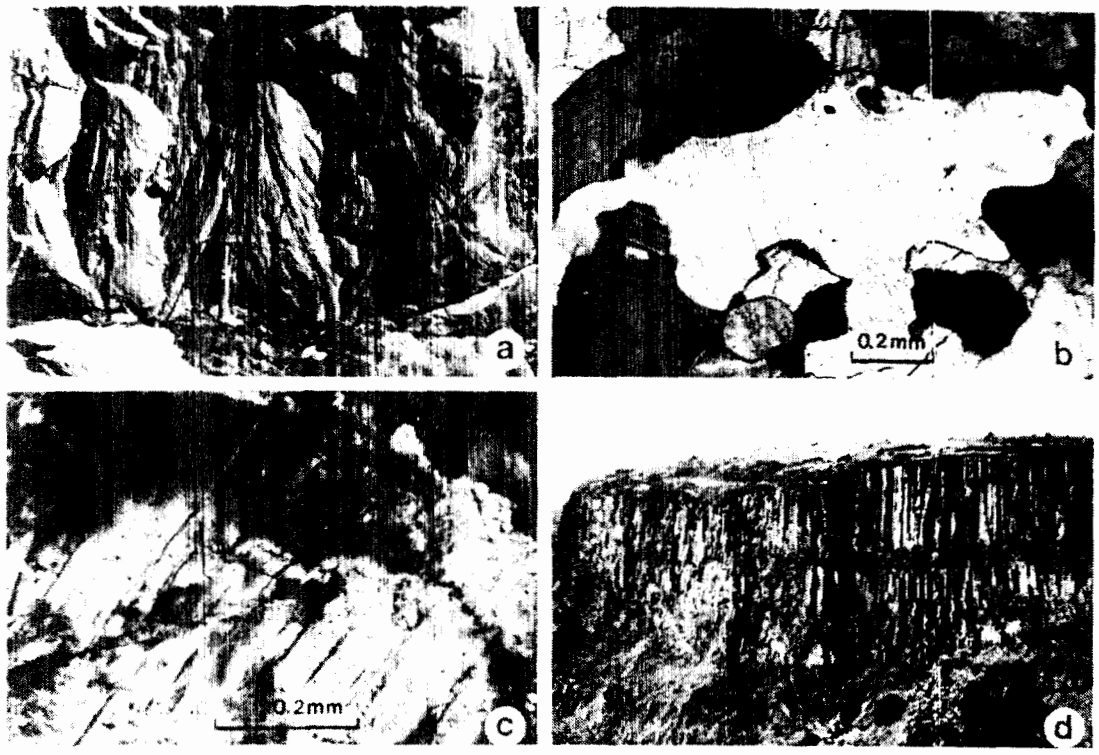

Figure 4 Shock-metamorphic features. (*a*) Shatter cones in quartzite, Sudbury, Ontario, Canada. (*b*) Microscopic planar features in quartz, Charlevoix, Quebec, Canada. Crossed polars. (*c*) Feldspar grain (grey) partially converted to diaplectic glass (black), Saint Martin, Manitoba, Canada. Crossed polars. (*d*) Erosional remnant of impact melt sheet at Mistastin, Newfoundland and Labrador, Canada. Cliff is ~80 m high.

(such as coesite) form in this pressure range. With increasing pressure, these glasses show signs of melting, so that by ~45–55 GPa many shocked rocks show evidence of flow, with inhomogeneous glasses corresponding to mixed mineral compositions.

Other silicates also show a progressive series of subsolidus shock-metamorphic effects involving the formation of planar features and or mechanical twins. Onset pressures are not as well documented by experimentation as they are for the tectosilicates, although pressure calibration is possible by comparison with shock features in coexisting tectosilicates. Observations of shock features in the autochthonous rocks at terrestrial impact structures indicate that the recorded shock pressures beneath simple structures are a maximum of ~25 GPa and decrease with depth (Robertson & Grieve 1977). At complex structures, maximum pressures of ~35 GPa are recorded in the centrally uplifted autochthonous rocks and decay radially and with depth (Dence 1968).

Above ~60 GPa, postshock temperatures are sufficient to cause whole-rock melting in the target, which leads to the formation of impact melt

rocks (Figure 4*d*). Melt rocks occur as pockets up to a few tens of meters thick in the breccia lens of simple structures, as coherent annular melt sheets up to several hundred meters thick surrounding central peaks in complex structures, as glassy bombs in ejecta deposits, and as glassy clasts in breccias and veins beneath the floors of impact structures. Impact melt rocks are characterized by a high degree of compositional homogeneity corresponding to a mixture of the target rocks, even when occurring in volumes of hundreds of cubic kilometers (Grieve & Floran 1978, Masaitis et al 1980). They are also characterized by considerable textural inhomogeneity, particularly when they occur as coherent sheets. Melt sheets are heavily charged with shocked and unshocked lithic and mineral clasts (>50%) at the top and bottom (Phinney et al 1978). Clast content decreases and matrix grain size increases toward the middle of impact melt sheets. Clasts are removed by resorption and reaction with the matrix melt, and their population is biased toward the more refractory lithologies and minerals.

The chemical homogeneity of melt sheets can be explained by their origin as a mixture of melted and vaporized target rocks, which are driven down into the expanding transient cavity under high-velocity turbulent flow. Textural inhomogeneity is due to the incorporation and later selective destruction of clasts and to variations in postimpact cooling history with vertical position in the melt sheet (Grieve et al 1977). Unlike igneous melts, impact melts are superheated. This is evidenced by their ability to remain liquid and resorb high contents of cold clasts (Onorato et al 1978) and by the occurrence of ultra-high-temperature breakdown minerals, such as baddelyite (El Goresy 1968).

In some cases, the melt rocks have higher K_2O/NaO ratios than the target rocks. This has led some to postulate that these rocks and their associated structures are the result of alkali igneous activity (Currie 1971). One possible explanation for this anomaly is selective elemental vaporization and condensation during melt and vapor formation (Basilevsky et al 1982). An alternative explanation is hydrothermal alteration (Dence 1971), particularly of highly shocked felsic clasts (Grieve 1978). This hypothesis is supported by experimentation, which indicates the rapid and total replacement of Na, and some Ca, by K in labradorite shocked to 26 GPa and exposed to KCl melt (Ostertag & Stöffler 1982).

Other excesses from average target-rock compositions have been noted for trace elements (such as Cr, Ni, and Co) at the parts per million level and other siderophiles (such as Ir) at the parts per billion level (Palme 1982, Basilevsky et al 1984). These enrichments represent the admixture of material from the impacting body. In some cases, the relative abundances of these elements in impact melt rocks has been used to identify

the composition of the impacting body to the meteoritic group level, e.g. LL chondrite at the Brent crater (Palme 1982). In other cases, however, specific identification of the type of impacting body is equivocal. Lack of siderophile element enrichments in melt rocks does not necessarily imply the absence of a component of the impacting body. The compositions of basaltic achondrites, some irons, and stony irons are such that a small component of meteoritic material cannot be detected above background target values. In addition, as the total amount of vapor and melt increases with the square of the impact velocity (O'Keefe & Ahrens 1977), particularly high-velocity events will effectively dilute the fraction of the impacting body in the melt, which is seldom greater than a few percent at best.

FORMATIONAL PROCESSES

From experiments (Gault et al 1968, Stöffler et al 1975), calculations (Maxwell 1977, Orphal 1977), and observations (Dence et al 1977, Masaitis et al 1980), the process of forming simple structures is fairly well understood. Details and quantified aspects of cratering mechanics can be found in Croft (1980), Melosh (1980), Basilevsky et al (1983), and Grieve & Garvin (1984). Target material is compressed and accelerated downward and outward at initial particle velocities of several kilometers per second by the shock wave. Rarefaction waves, generated at free surfaces (such as the rear of the impacting body and the ground surface), follow the compressional wave and restore the compressed target material to ambient pressure. The rarefaction wave fronts are not parallel to the compressional wave, except in the volume directly below the impacting body. Consequently, the particle accelerations associated with rarefaction lead to the deflection of the initial downward and outward particle motions to upward and outward motions for that portion of the target near the surface. This results in the excavation of target material. Thus a cratering flow field is established, and a cavity known as the transient cavity is formed, partly by upward and outward excavation and partly by downward and outward displacement (Figure 5).

Cavity reconstructions suggest that this transient cavity has a depth to diameter ratio of $\sim 1/3$ (Dence et al 1977). As its name suggests, the transient cavity is short lived. In fact, it may never truly exist as a physical entity at the moment in time when there is both maximum downward displacement and maximum radial excavation (Schultz et al 1981). Whatever the case, the cavity walls very rapidly collapse inward to form the breccia lens observed at simple structures (Figure 5). In the freshest

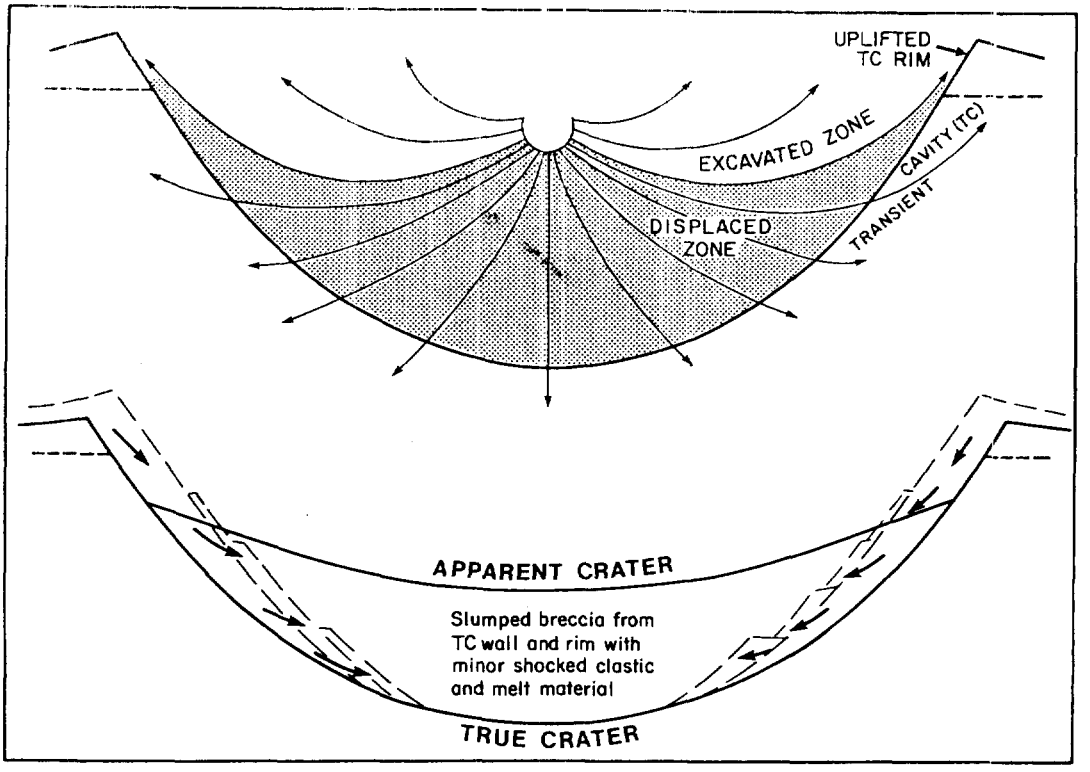

Figure 5 Formation of a simple crater. (*top*) Formation of transient cavity by a combination of excavation and displacement by the cratering flow field. Dashed line is original ground surface. (*bottom*) Subsequent collapse of transient cavity walls to form the final crater with allochthonous breccia lens. See text for details.

examples, this allochthonous breccia lens is overlain by a thin deposit of fallback breccia, which settles out of the ejecta cloud (Shoemaker 1960).

There is less consensus on the details of cratering mechanics at complex structures (Schultz & Merrill 1981). Difficulties in scaling small-scale experiments and extrapolating trends in computational models downgrade the constraints available. There is considerable observational evidence that morphologic features, such as uplifted central structures, indicate extensive structural movement. The majority of the models center on uplift and collapse hypotheses in which the original cavity produced by the cratering flow field undergoes considerable modification under plastic conditions (Melosh 1977; Figure 6). The driving force for modification has been considered to be gravity (Dence 1968, Melosh 1977) or a combination of gravity and elastic rebound (Ullrich et al 1977, Grieve & Robertson 1979).

The debate largely revolves around the validity of the concept of an initial deep transient cavity similar to that for simple structures (Roddy 1977, Pike 1980, Croft 1981). Data from terrestrial complex structures have been cited in favor of similar initial geometries (Dence et al 1977). Regardless of the details of transient cavity geometry, it is apparent that

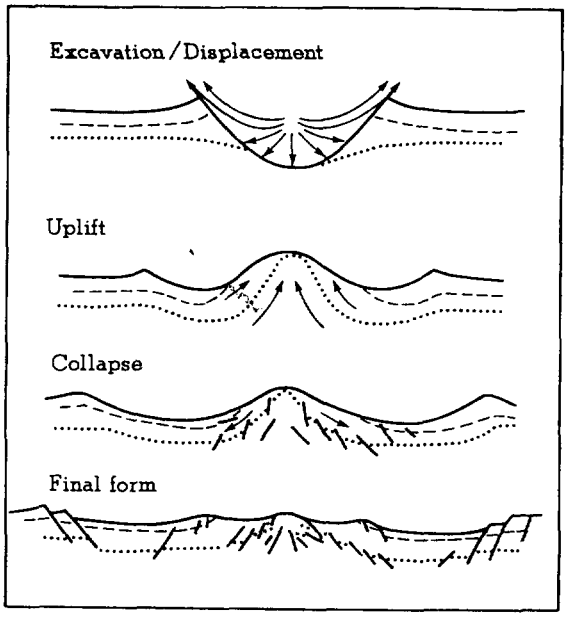

Figure 6 Model of the formation of a complex structure. Top to bottom represents increasing time following impact. Initial excavation and displacement is assumed to be similar to simple craters and is followed by considerable modification through uplift and collapse to produce the final form. See text for details.

deep excavation in complex structures is confined to the central region. The diameter of significant excavation is limited to 0.5–0.65 times the final diameter, which is determined by downfaulting during modification. Where there is sufficient control, estimates of the maximum depth of excavation indicate depths comparable to those of simple structures, provided they are normalized to the excavated rather than the final diameter (Grieve et al 1981). Observational data indicate the depth of excavation is $\sim 0.05D$. The question of the depth of excavation is particularly important in interpreting the provenance of lunar highland samples, which may be related to the formation of multiring impact basins, and in determining the effects of basin-sized events on lunar crustal stratigraphy (Spudis 1984).

THE KNOWN IMPACT RECORD

Small, young impact structures may have associated fragments of the impacting body, since relatively small bodies impact with reduced velocities due to atmospheric retardation or breakup (Melosh 1981). At larger structures, fragments of the impacting body are not expected, since the pressures and temperatures associated with undiminished impact velocities are sufficient to vaporize and melt the impacting body. The absence of physical

evidence of the impacting body coupled with complexities in crater form at larger diameters and the modifying effects of erosion have resulted in considerable historical controversy over the origin of many terrestrial impact structures. A variety of internal processes, such as cryptoexplosions of gas, have been cited (Bucher 1963). A considerable literature now exists on impact phenomena, however, such that only a few geologists question the existence of large terrestrial impact structures without associated meteorite fragments (McCall 1979). Recognition of new structures is no longer solely the province of experts in the field of impact processes, and new discoveries are now being made of the order of five per year.

On the basis of the recognition of meteorite fragments and/or shock-metamorphic features, the current listing of known terrestrial impact structures indicates ages from Precambrian to Recent and diameters from $D \sim 140$ km to a few tens of meters (Table 1). Known structures are restricted to the exposed land. Oceanic impact structures or their derivatives must exist, but the current level of detailed knowledge of ocean-floor topography and geology is insufficient to lead to the straightforward discovery of submarine impact structures. Although impact is a spatially random process, the location of known impact structures is not. The concentrations on the cratons of North America and Europe (Figure 7) are the result of the relatively long-term geologic stability and active study and search programs in these areas.

There is also a bias toward younger structures; over 50% of the known structures with $D > 10$ km have ages < 200 Myr (Table 1). This is the result of erosion, which can rapidly render the crater form and the underlying structurally disturbed target unrecognizable. The effect of erosion can be seen in the cumulative size-frequency distribution of terrestrial structures. For large diameters the distribution approximates the relation $N \propto D^{-1.8}$, where N is cumulative number (Figure 8). This relation is considered to be the crater production rate on the other terrestrial planets (Neukum & Wise 1976). At smaller diameters, however, the distribution falls off (Figure 8), which indicates the removal of craters by erosion and difficulties in recognizing small structures.

If crater preservation is considered in terms of the depth to which the effects of impact are visible, the geologic signature of structures with $D > 20$ km that have not been protected from erosion by postimpact sedimentation and that occur in glaciated areas can be removed in as little as ~ 100 Myr (Grieve 1984). It is important, therefore, when commenting on terrestrial cratering rates and their variability through time to remember that the known sample is not necessarily representative, and it may be necessary to consider subsamples with restricted sizes, ages, and erosional histories.

Table 1 Terrestrial impact structures

Name	Latitude	Longitude	Diameter (km)	Age (Myr)
Amguid, Algeria	26°05′N	004°23′E	0.45	<0.1
Aouelloul, Mauritania[a]	20°15′N	012°41′W	0.37	3.1±0.3
Araguainha Dome, Brazil	16°46′S	052°59′W	40	<250
Azuara, Spain	41°01′N	000°55′W	30	<130
Barringer, Arizona, USA[a]	35°02′N	111°01′W	1.2	0.025
Bee Bluff, Texas, USA	29°02′N	099°51′W	2.4	<40
Beyenchime-Salaatin, Russian SFSR, USSR	71°50′N	123°30′E	8	<65
Bigatch, Kazakh SSR, USSR	48°30′N	082°00′E	7	6±3
Boltysh, Ukraine, USSR	48°45′N	032°10′E	25	100±5
Bosumtwi, Ghana	06°32′N	001°25′W	10.5	1.3±0.2
Boxhole, Northern Territory, Australia[a]	22°37′S	135°12′E	0.18	—
B.P. Structure, Libya	25°19′N	024°20′E	2.8	<120
Brent, Ontaria, Canada[a]	46°05′N	078°29′W	3.8	450±30
Campo del Cielo, Argentina (20)[a,b]	27°38′S	061°42′W	0.09	—
Carswell, Saskatchewan, Canada	58°27′N	109°30′W	37	117±8
Charlevoix, Quebec, Canada	47°32′N	070°18′W	46	360±25
Clearwater Lake East, Quebec, Canada	56°05′N	074°07′W	22	290±20
Clearwater Lake West, Quebec, Canada	56°13′N	074°30′W	32	290±20
Connolly Basin, Western Australia, Australia	23°32′S	124°45′E	9	<60
Crooked Creek, Missouri, USA	37°50′N	091°23′W	5.6	320±80
Dalgaranga, Western Australia, Australia[a]	27°43′S	117°05′E	0.21	—
Decaturville, Missouri, USA	37°54′N	092°43′W	6	<300
Deep Bay, Saskatchewan, Canada	56°24′N	102°59′W	12	100±50
Dellen, Sweden	61°55′N	016°32′E	15	109.6±1
Eagle Butte, Alberta, Canada	49°42′N	110°30′W	10	<65
El'gygytgyn, Russian SFSR, USSR	67°30′N	172°05′E	23	3.5±0.5
Flynn Creek, Tennessee, USA	36°17′N	085°40′W	3.8	360±20
Glover Bluff, Wisconsin, USA	43°58′N	089°32′W	6	<500
Goat Paddock, Western Australia, Australia	18°20′S	126°40′E	5	<50
Gosses Bluff, Northern Territory, Australia	23°50′S	132°19′E	22	142.5±0.5
Gow Lake, Saskatchewan, Canada[a]	56°27′N	104°29′W	5	<250
Gusev, Russian SFSR, USSR	48°20′N	040°15′E	3	65

Name	Latitude	Longitude	Diameter (km)	Age (Myr)
Haughton, Northwest Territories, Canada	75°22′N	089°40′W	20	21.5±1.2
Haviland, Kansas, USA[a]	37°35′N	099°10′W	0.011	—
Henbury, Northern Territory, Australia (14)[a,b]	24°34′S	133°10′E	0.15	—
Holleford, Ontario, Canada	44°28′N	076°38′W	2	550±100
Ile Rouleau, Quebec, Canada	50°41′N	073°53′W	4	<300
Ilintsy, Ukraine, USSR	49°06′N	029°12′E	4.5	395±5
Ilumetsy, Estonia, USSR	57°58′N	025°25′E	0.08	0.002
Janisjärvi, Russian SFSR, USSR	61°58′N	030°55′E	14	698±22
Kaalijärvi, Estonia, USSR (7)[a,b]	58°24′N	022°40′E	0.11	0.004
Kaluga, Russian SFSR, USSR	54°30′N	036°15′E	15	380±10
Kamensk, Russian SFSR, USSR	48°20′N	040°15′E	25	65
Kara, Russian SFSR, USSR[a]	69°10′N	065°00′E	60	57±9
Karla, Russian SFSR, USSR	57°54′N	048°00′E	10	10
Kelly West, Northern Territory, Australia	19°30′S	132°50′E	2.5	<550
Kentland, Indiana, USA	40°45′N	087°24′W	13	<300
Kjardla, Estonia, USSR	57°00′N	022°42′E	4	510±30
Kursk, Russian SFSR, USSR	51°40′N	036°00′E	5	250±80
Lac Couture, Quebec, Canada	60°08′N	075°20′W	8	425±25
Lac La Moinerie, Quebec, Canada	57°26′N	066°36′W	8	400±50
Lappajärvi, Finland[a]	63°09′N	023°42′E	14	77±4
Liverpool, Northern Territory, Australia	12°24′S	134°03′E	1.6	150±70
Logancha, Russian SFSR, USSR	65°30′N	095°50′E	20	50±20
Logoisk, Byelorussia, USSR	54°12′N	027°48′E	17	40±5
Lonar, India	19°58′N	076°31′E	1.83	0.05
Machi, Russian SFSR, USSR (5)[b]	57°30′N	116°00′E	0.3	<1
Manicouagan, Quebec, Canada	51°23′N	068°42′W	100	210±4
Manson, Iowa, USA	42°35′N	094°31′W	32	61±9
Middlesboro, Kentucky, USA	36°37′N	083°44′W	6	<300
Mien, Sweden[a]	56°25′N	014°52′E	5	118±3
Misarai, Lithuania, USSR	54°00′N	023°54′E	5	395±145
Mishina Gora, Russian SFSR, USSR	58°40′N	028°00′E	2.5	<360
Mistastin, Newfoundland, and Labrador, Canada	55°53′N	063°18′W	28	38±4
Monturaqui, Chile[a]	23°56′S	068°17′W	0.46	1
Morasko, Poland (7)[a,b]	52°29′N	016°54′E	0.1	0.01

Table 1 (*continued*)

Name	Latitude	Longitude	Diameter (km)	Age (Myr)
New Quebec, Quebec, Canada	61°17′N	073°40′W	3.2	<5
Nicholson Lake, Northwest Territories, Canada[a]	62°40′N	102°41′W	12.5	<400
Oasis, Libya	24°35′N	024°24′E	11.5	—
Obolon', Ukraine, USSR[a]	49°30′N	032°55′E	15	215±25
Odessa, Texas, USA (3)[a,b]	31°45′N	102°29′W	0.168	—
Ouarkziz, Algeria	29°00′N	007°33′W	3.5	<70
Piccaninny, Western Australia, Australia	17°32′S	128°25′E	7	<360
Pilot Lake, Northwest Territories, Canada	60°17′N	111°01′W	6	440±2
Popigai, Russian SFSR, USSR[a]	71°30′N	111°00′E	100	39±9
Puchezh-Katunki, Russian SFSR, USSR	57°06′N	043°35′E	80	183±5
Red Wing Creek, North Dakota, USA	47°36′N	103°33′W	9	200
Riacho Ring, Brazil	07°43′S	046°39′W	4	—
Ries, Fed. Rep. Germany[a]	48°53′N	010°37′E	24	14.8±0.7
Rochechouart, France[a]	45°30′N	000°56′E	23	160±5
Rogozinskaja, Russian SFSR, USSR	58°18′N	062°00′E	8	55±5
Rotmistrovka, Ukraine, USSR	49°00′N	032°00′E	2.5	140±20
Sääksjärvi, Finland[a]	61°23′N	022°25′E	5	<330
Saint Martin, Manitoba, Canada	51°47′N	098°32′W	23	225±40
Serpent Mound, Ohio, USA	39°02′N	083°24′W	6.4	<320
Serra da Canghala, Brazil	08°05′S	046°52′W	12	<300
Shunak, Kazakh SSR, USSR	42°42′N	072°42′E	2.5	12
Sierra Madera, Texas, USA	30°36′N	102°55′W	13	100
Sikhote Alin, Russian SFSR, USSR (122)[a,b]	46°07′N	134°40′E	0.0265	—
Siljan, Sweden	61°02′N	014°52′E	52	368±1
Slate Island, Ontario, Canada	48°40′N	087°00′W	30	<350
Sobolev, Russian SFSR, USSR[a]	46°18′N	138°52′E	0.05	—
Söderfjärden, Finland	63°02′N	021°35′E	5.5	<600
Spider, Western Australia, Australia	16°30′S	126°00′E	5	—
Steen River, Alberta, Canada	59°31′N	117°38′W	25	95±7
Steinheim, Fed. Rep. Germany	48°41′N	010°04′E	3.4	14.8±0.7
Strangways, Northern Territory, Australia[a]	15°12′S	133°35′E	24	<472
Sudbury, Ontario, Canada	46°36′N	081°11′W	140	1850±150
Tabun-Khara-Obo, Mongolia[a]	44°06′N	109°36′E	1.3	<30
Talemzane, Algeria	33°19′N	004°02′E	1.75	<3

Name	Latitude	Longitude	Diameter (km)	Age (Myr)
Teague, Western Australia, Australia	25°50′S	120°55′E	28	1685±5
Tenoumer, Mauritania	22°55′N	010°24′W	1.9	2.5±0.5
Ternovka, Ukraine, USSR	48°01′N	033°05′E	8	330±30
Tin Bider, Algeria	27°36′N	005°07′E	6	<70
Ust-Kara, Russian SFSR, USSR	69°18′N	065°18′E	25	57±9
Upheaval Dome, Utah, USA	38°26′N	109°54′W	5	—
Veevers, Western Australia, Australia[a]	22°58′S	125°22′E	0.08	<450
Vepriaj, Lithuania, USSR	55°06′N	024°36′E	8	160±30
Vredefort, South Africa	27°00′S	027°30′E	140	1970±100
Wabar, Saudi Arabia (2)[a,b]	21°30′N	050°28′E	0.097	—
Wanapitei Lake, Ontaria, Canada[a]	46°44′N	080°44′W	8.5	37±2
Wells Creek, Tennessee, USA	36°23′N	087°40′W	14	200±100
West Hawk Lake, Manitoba, Canada	49°46′N	095°11′W	2.7	100±50
Wolf Creek, Western Australia, Australia[a]	19°10′S	127°47′E	0.85	—
Zeleny Gai, Ukraine, USSR	48°42′N	035°54′E	1.4	120±20
Zhamanshin, Kazakh SSR, USSR[a]	48°24′N	060°48′E	10	0.75±0.06

[a] Structures with meteoritic fragments or geochemical anomalies considered to have a meteoritic source.
[b] Sites with multiple craters, with (*n*) indicating number of craters. Diameter given corresponds to largest crater.

Cratering Rate Estimates

The ubiquitous nature of cratering in the solar system has resulted in the use of crater counts to estimate the age of unsampled planetary surfaces (Basaltic Volcanism Study Project 1981, pp. 1050–1129). Central to estimating absolute ages is knowledge of the crater production rate and its variation over geologic time for the planet in question. Estimates of the crater production rate with time depend on data from the Earth and Moon, the only bodies for which samples and thus ages are currently available. The lunar data are for relatively large numbers of structures on isotopically dated surfaces >3.0 Gyr. The terrestrial data are for relatively small numbers of structures with isotopic or biostratigraphic ages on relatively young surfaces.

It is insufficient, however, to simply count the number of craters greater than some size and older than some age to derive a terrestrial crater

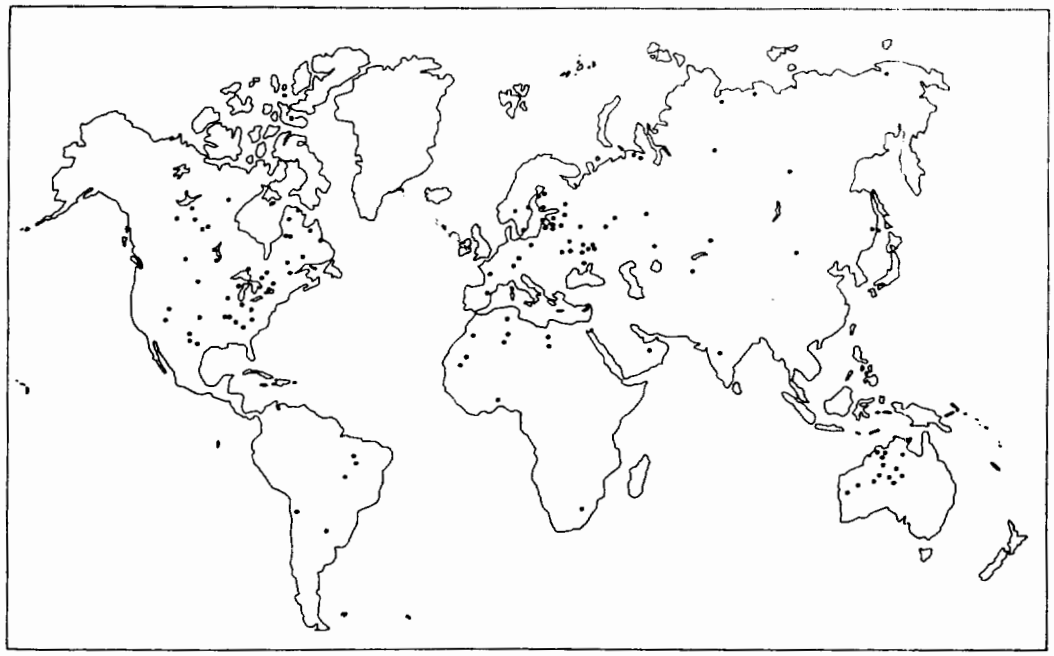

Figure 7 Location of known terrestrial impact structures.

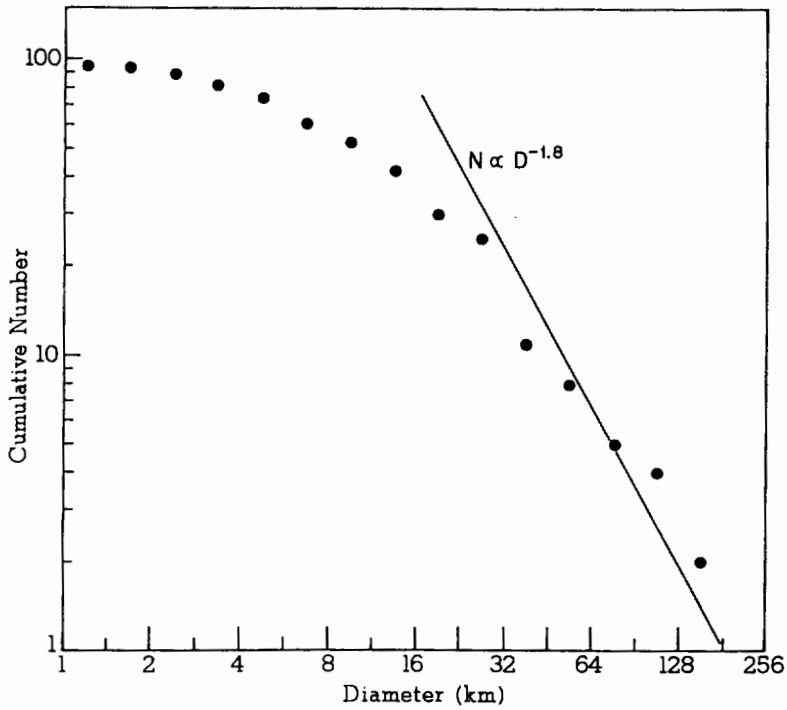

Figure 8 Cumulative size-frequency distribution of known terrestrial impact structures in Table 1. Note departure from $N \propto D^{-1.8}$ at smaller diameters, which indicates a shortage of known craters due to crater recognition and retention problems.

production rate. There are considerable uncertainties in many biostratigraphic ages, and there are also potential difficulties with K/Ar ages of impact melt rocks, which contain only partially degassed lithic and mineral clasts (Mak et al 1976). The major problems, however, are with crater recognition and retention. Average terrestrial cratering rate estimates have been calculated from well-dated, relatively young (<120 Myr) large craters on the North American and European cratons ($5.4 \pm 2.7 \times 10^{-15}$ km^{-2} yr^{-1} for $D \geq 20$ km, $n = 7$; Grieve 1984) and from smaller craters on a nonglaciated area in the United States with a well-established geologic history ($2.2 \pm 1.1 \times 10^{-14}$ yr^{-1} km^{-2} for $D \geq 10$ km, $n = 4$; Shoemaker 1977). For $N \propto D^{-1.8}$, these independent rate estimates are comparable and similar to that derived from observations on bodies with Earth-crossing orbits ($2.4 \pm 2.2 \times 10^{-14}$ km^{-2} yr^{-1} for $D \geq 10$ km; Shoemaker 1983). All estimates have large uncertainties, reflecting concerns over the small number of observations and the completeness of the searches.

LARGE-SCALE IMPACT AND TERRESTRIAL EVOLUTION

Planetary exploration missions have provided evidence that the terrestrial planets were subjected to an episode of heavy bombardment during their early history. Although clear evidence of this episode is lacking on Earth and possibly Venus (Ivanov et al 1986), the question remains whether it had any lasting effect on terrestrial evolution. If a terrestrial crust and lithosphere did exist during the heavy bombardment, the potential numbers of impact structures can be estimated from the cratering record in the lunar highlands. After corrections for the larger gravitational cross section, higher impact velocity, and stronger gravity of the Earth, estimates for the number of potential impact basins with $D \geq 1000$ km range from 30–60 to 200 (Frey 1980, Grieve & Parmentier 1984). Estimated parameters such as the addition of exogenic energy and impact melt production on the early Earth, when averaged over the several hundred million years of bombardment, are of the same order of magnitude as present-day internal energy losses and island-arc volcanism (Grieve 1980). There is, however, a fundamental difference in the mode of energy release. Each major impact deposited orders of magnitude more energy than present-day internal energy losses at a specific location on time scales that are essentially instantaneous.

The immediate consequences of a basin-sized event would have been the establishment of topography on the order of a few kilometers, disturbance of the subimpact thermal gradient by the addition of postshock

waste heat, and the uplift of originally deep-seated materials and considerable crustal fracturing. The combination of excavation, uplift, and a relatively thin lithosphere raises the possibility of impact-induced volcanism resulting from lithospheric thinning or removal and adiabatic decompression. Such a sequence has been suggested to account for the occurrence of the 1.85-Gyr-old Sudbury Igneous Complex (French 1970), and consideration of these effects led Frey (1980) to postulate that basin-sized impacts could produce proto-ocean basins and thus the basic crustal dichotomy of the Earth.

A number of processes would act to modify these impact basins (e.g. thermal subsidence, topographic degradation by erosion, and relaxation and basin loading). Some of these effects have been modeled for lunar basins with the result that lunar basins appear to have appreciable effects for 10^6–10^8 yr on the thermal, tectonic, and volcanic history in and around the basin (Bratt et al 1985, Solomon et al 1982). Calculations for a model 1000-km basin on an early Earth indicates conductive heat losses for 10^7 yr and postimpact thermal and isostatic subsidence of $\sim$5–6 km (Grieve & Parmentier 1984). This time scale is similar to that for the Moon but does not account for the more vigorous heat losses associated with convection, which are likely in the terrestrial case. While it is clear that such basin-sized events would have appreciable direct and indirect effects on the early crust and lithosphere, it is not yet clear that they would be sufficiently long lived to significantly affect early crustal evolution.

Some authors have suggested relationships between more recent large impacts and such phenomena as magnetic reversals and plate movements (Glass et al 1979, Clube & Napier 1982). These suggestions remain unproven. It has also been suggested that large-scale impact may have been responsible for certain mass extinctions in the geologic record (de Laubenfels 1956, McClaren 1970). Evidence in favor of this hypothesis was first presented by Alvarez et al (1980) and Ganapathy (1980) in the form of relatively high abundances of Ir and other siderophile elements in the Cretaceous-Tertiary boundary clay layer at Gubbio, Italy, Stevns Klint, Denmark, and Woodside, New Zealand. Since these initial discoveries, numerous workers have confirmed a global enrichment in siderophile elements at Cretaceous-Tertiary boundary sites. Other evidence in favor of a major impact is the roughly chondritic abundances for the siderophiles (Kyte et al 1985), with isotopic data indicating that the boundary layer is distinct from normal detrital sediments (DePaolo et al 1983) and suggesting a meteoritic source (Luck & Turekian 1983). Physical evidence for an impact is given by the occurrence of shocked quartz and feldspar (Bohor et al 1984, Izett & Pillmore 1985), sanidine and microtektite spherules (Smit & Klaver 1981, Graup et al 1986), and high-temperature spinels

(Smit & Kyte 1984) at boundary-layer sites. The evidence is consistent with the global dispersion of projectile-contaminated, early-time ejecta from a major impact event (O'Keefe & Ahrens 1982). Mass-balance calculations suggest a projectile mass of 10^{17}–10^{18} g with associated kinetic energy of $\sim 10^{23}$ J. There is no known structure commensurate in both size ($\sim$100–200 km) and age ($\sim$65 Myr) with the values required for such an impact. This is not necessarily a fatal flaw in the hypothesis, as isotopic data suggest the presence of basaltic crustal materials within the boundary layer, implying an oceanic impact (DePaolo et al 1983).

A number of impact-induced extinction mechanisms have been suggested. The first is high dust loading of the stratosphere leading to the cessation of photosynthesis and breakdown of the food chain (Alvarez et al 1980). Model calculations suggest that light levels would be reduced below that required for photosynthesis for several months, and that there would be protracted cooling of the land surface (Pollack et al 1983). Another possibility is short-term heating of the atmosphere due to a greenhouse effect induced by water vapor from an oceanic impact (Emiliani et al 1981). Finally, the extinctions could have been induced through poisoning by noxious chemicals (Hsü 1980) or by the creation of large quantities of oxides of nitrogen by shock heating of the atmosphere, resulting in highly acidic rains (Lewis et al 1982). The hypothesis of impact-induced extinctions at the Cretaceous-Tertiary boundary has not gone unchallenged. Alternate hypotheses centering mainly on large-scale volcanism have been offered (McLean 1985, Officer & Drake 1985). Although there are still considerable uncertainties with respect to the details of the Cretaceous-Tertiary event, the observational evidence is consistent with the occurrence of a major impact, and thus an impact-related mass extinction remains a good working hypothesis.

Searches are currently underway for other siderophile anomalies in the geologic record. A correlation between microtektites, anomalous Ir, and the extinction of some late Eocene radiolaria has been reported (Sanfilippo et al 1985). An Ir anomaly has been detected in the Upper Devonian near the Frasnian-Famennian boundary, but it is possible that this anomaly has a terrestrial source (Playford et al 1984). There are also claims of Ir anomalies at the Permo-Triassic and Cambrian-Precambrain boundaries, but these results are preliminary.

It is tempting to speculate that large-scale impact was the forcing function for a number of, or possibly all, mass extinctions. Raup & Sepkoski (1984) statistically analyzed the marine extinction record over the last 250 Myr and determined a periodicity of 26 Myr with a phase of 13 Myr. A number of authors have suggested that periodic cometary showers, resulting from perturbations of the Oort cloud (the outer solar system

source of comets) by an unseen solar companion or passage of the solar system through the galactic plane, could account for the periodic mass extinctions. Evidence in favor of periodic impacts has been presented through analyses of the ages of known craters by Alvarez & Muller (1984) and Rampino & Stothers (1984). They determined periodicities of 28.4 ± 1 Myr with a phase of 13 ± 2 Myr and 31 ± 1 Myr with a phase of 5 ± 6 Myr, respectively. From a review of the record, however, Grieve et al (1985) concluded that, because of its inherent nature, there were considerable uncertainties in using time-series analyses on the cratering record, and that a variety of periods could be defined depending on which sample of the record was considered most representative. They also argued that siderophile data suggested a variety of projectile types were responsible for the analyzed craters, and that the similarity in the cratering rate as determined from known craters and from observations of Earth-crossing Apollo bodies argued against periodic cometary showers.

SUMMARY

Approximately 120 terrestrial impact structures are currently known and several new structures are recognized each year. They are characterized by a circular form, severe surface and near-surface structural disturbance, and the occurrence of shock-metamorphic features. Projectile fragments are restricted to the smaller young structures, but larger structures may contain meteoritic material in the form of enriched siderophile abundances in impact melt rocks. The cratering process is fairly well understood for simple structures, but details for complex structures ($D > 4$ km) are less clear and additional work is required. Impact is a ubiquitous process in the solar system, and terrestrial impact structures provide the only ground-truth to understand large-scale impact as a geologic process. Consequently, recent research has centered less on the identification of new structures and more on the observational constraints terrestrial impact structures can provide to an understanding of impact phenomena. Unlike bodies such as the Moon, there is no clear evidence that large-scale impact had a lasting effect on the early crustal evolution of the Earth during the period of heavy bombardment. Modeling to date suggests fairly long-lived thermal and tectonic effects, but these models are preliminary.

There is good circumstantial evidence that a more recent large-scale impact affected severely the biosphere at the Cretaceous-Tertiary boundary. Details, however, of the killing mechanism(s) and the exact nature of the impact event still require research. There are some suggestions that large-scale impact was related to other global extinction events in the geologic record, but at present these are poorly documented; thus,

categorical statements regarding terrestrial impact and other mass extinctions are premature. Similarly, suggestions that the Earth is subjected to periodic cometary showers require evidence beyond statistical arguments based on an incomplete cratering record. The potential for a relationship between large-scale impact events and climatological and biological changes is exciting and may ultimately result in a reevaluation of current thinking. Much work, however, remains to be done before large-scale impact can be considered the panacea for questions related to rapid changes in terrestrial biological evolution.

ACKNOWLEDGMENTS

This article is Geological Survey of Canada Contribution No. 21586.

Literature Cited

Alvarez, L. W., Alvarez, W., Asaro, F., Michel, H. V. 1980. Extraterrestrial cause for the Cretaceous-Tertiary extinction. *Science* 208: 1095–1108

Alvarez, W., Muller, R. A. 1984. Evidence from crater ages for periodic impacts on the Earth. *Nature* 308: 718–20

Basaltic Volcanism Study Project. 1981. *Basaltic Volcanism on the Terrestrial Planets*. New York: Pergamon. 1286 pp.

Basilevsky, A. T., Florensky, K. P., Yakolev, O. I., Ivanov, B. A., Fel'dman, V. I., Granovsky, L. B. 1982. Transformation of planetary material in high-speed collisions. *Geokhimiya* 1982(7): 946–60 (In Russian)

Basilevsky, A. T., Ivanov, B. A., Florensky, K. P., Yakolev, O. I., Fel'dman, V. I., et al. 1983. *Impact Craters on the Moon and Planets*. Moscow: Nauka. 200 pp. (In Russian)

Basilevsky, A. T., Fel'dman, V. I., Kapustkina, I. G., Kolesov, G. M. 1984. On the distribution of iridium in the rocks of terrestrial impact craters. *Geokhimiya* 1984(6): 781–90 (In Russian)

Bohor, B. F., Frood, E. E., Modreski, P. J., Triplehorn, D. M. 1984. Mineralogic evidence for an impact event at the Cretaceous-Tertiary boundary. *Science* 224: 867–69

Bratt, S. R., Solomon, S. C., Head, J. W. 1985. The evolution of impact basins: cooling, subsidence and thermal stress. *J. Geophys. Res.* 90: 12,415–33

Brenan, R. L., Peterson, B. L., Smith, H. J. 1975. The origin of Red Wing Creek structure, McKenzie County, North Dakota. *Wyo. Geol. Assoc. Earth Sci. Bull.* 8(3): 1–41

Bucher, W. H. 1963. Cryptoexplosion structures caused from without or within the Earth? ("Astroblemes" or "Geoblemes"). *Am. J. Sci.* 261: 596–649

Clube, S. V. M., Napier, W. M. 1982. The role of episodic bombardment in geophysics. *Earth Planet. Sci. Lett.* 57: 251–62

Coles, R. L., Clark, J. F. 1978. The central magnetic anomaly, Manicouagan structure, Quebec. *J. Geophys. Res.* 83: 2805–8

Croft, S. K. 1980. Cratering flow fields: implications for the excavation and transient expansion stages of crater formation. *Proc. Lunar Planet. Sci. Conf., 11th*, pp. 2347–78

Croft, S. K. 1981. The excavation stage of basin formation: a qualitative model. See Schultz & Merrill 1981, pp. 207–26

Currie, K. L. 1971. A study of potash fenitization around the Brent crater, Ontario, a Paleozoic alkaline complex. *Can. J. Earth Sci.* 8: 481–97

Dabizha, A. I., Ivanov, B. A. 1978. A geophysical model of the structure of meteorite craters and problems of the mechanics of crater formation. *Meteoritika* 37: 160–67 (In Russian)

de Laubenfels, M. W. 1956. Dinosaur extinction: one more hypothesis. *J. Paleontol.* 30: 207–18

Dence, M. R. 1968. Shock zoning at Canadian craters: petrography and structural implications. See French & Short 1968, pp. 169–84

Dence, M. R. 1971. Impact melts. *J. Geophys. Res.* 76: 5525–65

Dence, M. R., Grieve, R. A. F., Robertson, P. B. 1977. Terrestrial impact structures:

principal characteristics and energy considerations. See Roddy et al 1977, pp. 247–76

DePaolo, D. J., Kyte, F. T., Marshall, B. D., O'Neil, J. R., Smit, J. 1983. Rb-Sr, Sm-Nd, K-Ca, O and H isotopic study of Cretaceous-Tertiary boundary sediments, Caravaca, Spain: evidence for an oceanic impact. *Earth Planet. Sci. Lett.* 64: 356–73

El Goresy, A. 1968. The opaque minerals in impactite glasses. See French & Short 1968, pp. 531–53

Emiliani, C., Kraus, E. B., Shoemaker, E. M. 1981. Sudden death at the end of the Mesozoic. *Earth Planet. Sci. Lett.* 55: 317–34

French, B. M. 1970. Possible relations between meteorite impact and igneous petrogenesis, as indicated by the Sudbury structure, Ontario, Canada. *Bull. Volcanol.* 34: 466–517

French, B. M., Short, N. M., eds. 1968. *Shock Metamorphism of Natural Materials*. Baltimore: Mono. 644 pp.

Frey, H. 1980. Crustal evolution of the early Earth: the role of major impacts. *Precambrian Res.* 10: 195–216

Ganapathy, R. 1980. A major meteorite impact on the Earth 65 million years ago: evidence from the Cretaceous-Tertiary boundary clay. *Science* 209: 921–23

Gault, D. E., Quaide, W. L., Oberbeck, V. R. 1968. Impact cratering mechanics and structure. See French & Short 1968, pp. 87–99

Glass, B. P., Swincki, M. B., Zwart, P. A. 1979. Australasian, Ivory Coast and North American tektite strewnfields: size, mass and correlation with geomagnetic reversals and other Earth events. *Proc. Lunar Planet. Sci. Conf., 10th*, pp. 2535–45

Graup, G., Huth, J., Rast, U., Spettel, B. 1986. Microtektites at the Cretaceous-Tertiary boundary. *Lunar Planet Sci. XVII*, pp. 283–84 (Abstr.)

Grieve, R. A. F. 1978. The melt rocks at Brent crater, Ontario. *Proc. Lunar Planet Sci. Conf., 9th*, pp. 2579–2608

Grieve, R. A. F. 1980. Impact bombardment and its role in proto-continental growth on the early Earth. *Precambrian Res.* 10: 217–48

Grieve, R. A. F. 1984. The impact cratering rate in recent time. *J. Geophys. Res.* 89: B403–8 (Suppl.)

Grieve, R. A. F., Floran, R. J. 1978. Manicouagan impact melt, Quebec. 2. Chemical interrelations with basement and formational processes. *J. Geophys. Res.* 83: 2761–71

Grieve, R. A. F., Garvin, J. B. 1984. A geometric model for excavation and modification at terrestrial simple impact craters. *J. Geophys. Res.* 89: 11,561–72

Grieve, R. A. F., Parmentier, E. M. 1984. Impact phenomena as factors in the evolution of the Earth. *Proc. Int. Geol. Congr., 27th, Moscow*, 19: 99–114. Utrecht: VNU Science

Grieve, R. A. F., Robertson, P. B. 1979. The terrestrial cratering record: I. Current status of observations. *Icarus* 38: 211–29

Grieve, R. A. F., Dence, M. R., Robertson, P. B. 1977. Cratering processes: as interpreted from the occurrence of impact melts. See Roddy et al 1977, pp. 791–814

Grieve, R. A. F., Robertson, P. B., Dence, M. R. 1981. Constraints on the formation of ring impact structures based on terrestrial data. See Schultz & Merrill 1981, pp. 37–57

Grieve, R. A. F., Sharpton, V. L., Goodacre, A. K., Garvin, J. B. 1985. A perspective on the evidence for periodic cometary impacts on Earth. *Earth Planet. Sci. Lett.* 76: 1–9

Hörz, F. 1968. Statistical measurements of deformation structures and refractive indices in experimentally shock loaded quartz. See French & Short 1968, pp. 243–54

Hsü, K. 1980. Terrestrial catastrophe caused by cometary impact at the end of the Cretaceous. *Nature* 285: 201–3

Ivanov, B. A., Basilevsky, A. T., Kryuchkov, V. P., Chernaya, I. M. 1986. Impact craters on Venus: analysis of Venera 15 and 16 data. *J. Geophys. Res.* 91: D413–30 (Suppl.)

Izett, G. A., Pillmore, C. L. 1985. Shock-metamorphic minerals at the Cretaceous-Tertiary boundary, Raton Basin, Colorado and New Mexico provide evidence for an asteroidal impact in continental crust. *Eos, Trans. Am. Geophys. Union* 66: 1149–50 (Abstr.)

Kyte, F. T., Smit, J., Wasson, J. T. 1985. Siderophile interelement variations in the Cretaceous-Tertiary boundary sediments from Caravaca, Spain. *Earth Planet Sci. Lett.* 73: 183–95

Lewis, J. S., Watkins, G. H., Hartman, H., Prinn, R. G. 1982. Chemical consequences of major impact events on Earth. *Geol. Soc. Am. Spec. Pap. No. 190*, pp. 215–22

Luck, J. M., Turekian, K. K. 1983. Osmium-187/Osmium-186 in manganese nodules and the Cretaceous-Tertiary boundary. *Science* 222: 613–15

Mak, E. K., York, D. E., Grieve, R. A. F., Dence, M. R. 1976. The age of the Mistastin Lake crater, Labrador, Canada. *Earth Planet. Sci. Lett.* 31: 345–57

Masaitis, V. L., Danilin, A. N., Mashchak,

M. S., Raykhlin, A. I., Selivanoskaya, T. V., Shadenkov, Y. E. M. 1980. *The Geology of Astroblemes*. Leningrad: Nedra. 231 pp. (In Russian)
Maxwell, D. E. 1977. Simple *Z* model of cratering, ejection and overturned flap. See Roddy et al 1977, pp. 1003–8
McCall, G. J. H., ed. 1979. *Astroblemes—Cryptoexplosion Structures. Benchmark Papers in Geology*, Vol. 50. Stroudsburg, Pa: Dowden, Hutchinson & Ross. 437 pp.
McClaren, D. J. 1970. Time, life and boundaries. *J. Paleontol.* 44: 801–15
McLean, D. M. 1985. Deccan traps mantle degassing in the terminal Cretaceous marine extinctions. *Cretaceous Res.* 6: 235–59
Melosh, H. J. 1977. Crater modification by gravity: a mechanical analysis of slumping. See Roddy et al 1977, pp. 1245–60
Melosh, H. J. 1980. Cratering mechanics—observational, experimental, and theoretical. *Ann. Rev. Earth Planet. Sci.* 8: 65–93
Melosh, H. J. 1981. Atmospheric breakup of terrestrial impactors. See Schultz & Merrill 1981, pp. 29–36
Milton, D. J. 1977. Shatter cones—an outstanding problem in shock mechanics. See Roddy et al 1977, pp. 703–14
Müller, W. F., Défourneaux, W. 1968. Deformation structures in quartz as an indicator for shock: an experimental study on crystalline quartz. *Z. Geophys.* 34: 483–504 (In German)
Neukum, G., Wise, D. U. 1976. Mars: a standard crater curve and possible new time scale. *Science* 194: 1381–87
Officer, C. B., Drake, C. L. 1985. Terminal Cretaceous environmental effects. *Science* 227: 1161–67
O'Keefe, J. D., Ahrens, T. J. 1977. Impact-induced energy partitioning, melting, and vaporization on terrestrial planets. *Proc. Lunar Sci. Conf., 8th*, pp. 3357–71
O'Keefe, J. D., Ahrens, T. J. 1982. The interaction of the Cretaceous-Tertiary bolide with the atmosphere, ocean and solid Earth. *Geol. Soc. Am. Spec. Pap. No. 190*, pp. 103–20
Onorato, P. I. K., Uhlmann, D. R., Simonds, C. H. 1978. The thermal history of the Manicouagan impact melt sheet, Quebec. *J. Geophys. Res.* 83: 2789–98
Orphal, D. L. 1977. Calculations of explosion cratering—II. Cratering mechanics and phenomenology. See Roddy et al 1977, pp. 907–17
Ostertag, R. 1983. Shock experiments on feldspar crystals. *J. Geophys. Res.* 88: B364–76 (Suppl.)
Ostertag, R., Stöffler, D. 1982. Thermal annealing of experimentally shocked feldspar crystals. *J. Geophys. Res.* 87: A457–64 (Suppl.)
Palme, H. 1982. Identification of projectiles at large terrestrial impact craters and some implications of Ir-rich Cretaceous-Tertiary boundary layers. *Geol. Soc. Am. Spec. Pap. No. 190*, pp. 223–33
Phinney, W. C., Simonds, C. H., Cochran, A., McGee, P. E. 1978. West Clearwater, Quebec, impact structure, part II: petrology. *Proc. Lunar Planet Sci. Conf., 9th*, pp. 2659–93
Pike, R. J. 1980. Formation of complex impact craters: evidence from Mars and other planets. *Icarus* 43: 1–19
Pike, R. J. 1985. Some morphologic systematics of complex impact structures. *Meteoritics* 20: 49–68
Playford, P. E., McClaren, D. J., Orth, C. J., Gilmore, J. S., Goodfellow, W. D. 1984. Iridium anomaly in the Upper Devonian of the Canning Basin, Western Australia. *Science* 226: 437–39
Pohl, J., Stöffler, D., Gall, H., Ernstson, K. 1977. The Ries impact crater. See Roddy et al 1977, pp. 343–404
Pollack, J. B., Toon, O. B., Ackerman, T. P., McKay, C. P., Turco, R. P. 1983. Environmental effects of an impact-generated dust cloud: implications for the Cretaceous-Tertiary extinctions. *Science* 219: 287–89
Rampino, M. R., Stothers, R. B. 1984. Terrestrial mass extinction, cometary impact and the Sun's motion perpendicular to the galactic plane. *Nature* 308: 709–12
Raup, D. M., Sepkoski, J. J. 1984. Periodicity of extinctions in the geologic past. *Proc. Natl. Acad. Sci. USA* 81: 801–5
Robertson, P. B. 1975. Experimental shock metamorphism of maximum microcline. *J. Geophys. Res.* 80: 1903–10
Robertson, P. B., Grieve, R. A. F. 1977. Shock attenuation at terrestrial impact structures. See Roddy et al 1977, pp. 687–702
Roddy, D. J. 1977. Pre-impact conditions and cratering processes at the Flynn Creek crater, Tennessee. See Roddy et al 1977, pp. 277–308
Roddy, D. J., Davis, L. K. 1977. Shatter cones formed in large-scale experimental explosion craters. See Roddy et al 1977, pp. 715–50
Roddy, D. J., Pepin, R. O., Merrill, R. B., eds. 1977. *Impact and Explosion Cratering*. New York: Pergamon. 1301 pp.
Sanfilippo, A., Riedel, W. R., Glass, B. P., Kyte, F. T. 1985. Late Eocene microtektites and radiolarian extinctions on Barbados. *Nature* 314: 613–15
Schneider, E., Wagner, G. W. 1976. Shatter cones produced experimentally by impacts in limestone targets. *Earth Planet. Sci. Lett.* 32: 40–44

Schultz, P. H., Merrill, R. B., eds. 1981. *Multi-Ring Basins*. New York: Pergamon. 295 pp.
Schultz, P. H., Orphal, D. L., Miller, B., Borden, W. F., Larson, S. A. 1981. See Schultz & Merrill 1981, pp. 181–95
Shoemaker, E. M. 1960. Penetration of high velocity meteorites, illustrated by Meteor Crater, Arizona. *Int. Geol. Congr., 21st, Copenhagen*, 18: 418–34
Shoemaker, E. M. 1977. Astronomically observable crater-forming projectiles. See Roddy et al 1977, pp. 617–28
Shoemaker, E. M. 1983. Asteroid and comet bombardment of the Earth. *Ann. Rev. Earth Planet. Sci.* 11: 461–94
Smit, J., Klaver, G. 1981. Sanidine spherules at the Cretaceous-Tertiary boundary indicate a large impact event. *Nature* 292: 47–49
Smit, J., Kyte, F. T. 1984. Siderophile-rich magnetic spheroids from the Cretaceous-Tertiary boundary in Umbria, Italy. *Nature* 310: 403–5
Solomon, S. C., Comer, R. P., Head, J. W. 1982. The evolution of impact basins: viscous relaxation of topographic relief. *J. Geophys. Res.* 87: 3975–92
Spudis, P. 1984. Apollo 16 site geology and impact melts: implications for the geologic history of the lunar highlands. *J. Geophys. Res.* 89: C95–107 (Suppl.)
Stöffler, D. 1972. Deformation and transformation of rock-forming minerals by natural and experimental shock processes. I. Behaviour of minerals under shock compression. *Fortschr. Mineral.* 49: 50–113
Stöffler, D. 1974. Deformation and transformation of rock-forming minerals by natural and experimental shock processes. II. Physical properties of shocked minerals. *Fortschr. Mineral.* 51: 256–89
Stöffler, D., Hornemann, U. 1972. Quartz and feldspar glass produced by natural and experimental shock. *Meteoritics* 7: 371–94
Stöffler, D., Gault, D. E., Wedekind, J., Polkowski, G. 1975. Experimental hypervelocity impact into quartz sand: distribution and shock metamorphism of ejecta. *J. Geophys. Res.* 80: 4062–77
Ullrich, G. W., Roddy, D. J., Simmons, G. 1977. Numerical simulations of a 20-ton TNT detonation on the Earth's surface and implications concerning the mechanics of central uplift formation. See Roddy et al 1977, pp. 959–83
von Engelhardt, W., Bertsch, W. 1969. Shock induced planar deformation structures in quartz from the Ries crater, Germany. *Contrib. Mineral. Petrol.* 20: 203–34
Wood, C. A., Head, J. W. 1976. Comparison of impact basins on Mercury, Mars, and the Moon. *Proc. Lunar Sci. Conf., 7th*, pp. 3629–51